Structural and Electrical Properties of Composites Based on Ni and NiAl Alloys for SOFC Application

S. M. Pikalov, E. Yu. Pikalova, and V. G. Bamburov

1 Introduction

To date, in an effort to increase the efficiency of solid oxide fuel cells (SOFCs), thin film fabrication methods have been extensively used. With all conventional techniques such as tape casting, screen printing and deep coating, the necessary application of high temperatures leads to an appearance of various defects in the case of large area cells and remarkable interaction between the functional layers at the production stage. Along with high deposition rates of materials, the main advantages of the air plasma spraying (APS) method in applying for electrode-supported SOFC fabrication, excluding the firing processes, are ease of control of component composition and microstructure and the ability to produce cells in a variety of different shapes [1].

Ni-YSZ composite anodes possess advanced catalytic and electrical properties and are known to have good compatibility with solid-state electrolytes based on ZrO_2, CeO_2, $LaGaO_3$ and $BaCeO_3$ [2]. Regardless of their drawbacks and the numerous investigations searching for new SOFC anodes, Ni-YSZ still remains a benchmark material in this field due to a lack of alternative high-performance anodes. The matter of long-term stability of Ni-cermet is directly connected with

S. M. Pikalov
Institute of Metallurgy, UB RAS, Yekaterinburg, Russia

E. Y. Pikalova (✉)
Institute of High Temperature Electrochemistry, UB RAS, Yekaterinburg, Russia

Department of Environmental Economics, Ural Federal University, Yekaterinburg, Russia

V. G. Bamburov
Department of Environmental Economics, Ural Federal University, Yekaterinburg, Russia

Institute of Solid State Chemistry, UB RAS, Yekaterinburg, Russia

S. Syngellakis, C. Brebbia (eds.), *Challenges and Solutions in the Russian Energy Sector*, Innovation and Discovery in Russian Science and Engineering,
https://doi.org/10.1007/978-3-319-75702-5_19

the anode's structure, uniformity of the distribution of Ni particles (preferable nanosized) into the ceramic matrix and the prevention of their coarsening. In addition to particle size and the Ni/ceramic component ratio, another important influencing factor on the coarsening of Ni particles in cermet is wettability, and this is strongly affected by the composition of the ceramic component. In Ref. [3] the functional properties of NiO-ScSZ anodes were improved by using the additive oxides MgO and Al_2O_3. It was reported that small Ni particles formed during anode reduction were stable against coarsening. In Ref. [4] it was shown that small additives of Al_2O_3 considerably improve the long-term stability of Ni-scandia-stabilized zirconia (ScSZ) anodes. A small amount of $NiAl_2O_4$ was found to have formed at the interface of NiO and Al_2O_3 during the anode sintering, and, after reducing, Ni particles were fixed in the ScSZ ceramic matrix by the $NiAl_2O_4$ and the defect spinel phase of $NiAl_{10}O_{16}$. The composite configuration prevented aggregation of Ni particles under operating conditions and provided stability of the anode structure and excellent electrical properties. Interesting results were presented in Ref. [5], where a single SOFC with a thin film YSZ electrolyte formed on a supported anode on a base of NiAl strain-reinforced alloy demonstrated improved performance (500 mW/cm^2 at 700 °C) and stable anode resistance (6–10 $\times$ 10^{-3} Ω $\times$ cm at 600 °C in a gas mixture of Ar/2–3%H_2 for a minimum of 300 h).

Intermetallides of NiAl system are widely used in different high-temperature applications owing to their properties such as high melting temperature, high creep strength, high corrosion and oxidation resistance [6]. In the present work, Ni and NiAl alloys were used as the components of the composites on a base of YSZ or Al_2O_3 ceramic powders. The structural, electrical and thermal properties of composites sprayed using the APS method and thermally treated in different atmospheres were investigated in terms of their prospective usage as anodes in SOFC and other electrochemical devices.

2 Experimental Details

2.1 Feedstock Powders

As the feedstock powders for the production of the composite materials, flowable Ni powder of 20–80 μm fraction (Norilsk Nickel, Russia) or NiAl (Al-clad Ni with Al content of 5% ($Ni_{95}Al_5$) and 15% ($Ni_{85}Al_{15}$), Tulachermet, Russia) and α-$A1_2O_3$ (Al_2O_3 content of no less than 99%, RUSAL, Russia) or 9.5YSZ (ZrO_2 stabilized by 9.5 mol.% Y_2O_3, Titov's lab firm, Yekaterinburg, Russia) of regular spherical shape with a mean particle size of 50 μm and a flowing rate of 60 g/min were used. According to XRD (diffractometer DMAX-2500) 9.5YSZ has a cubic structure (Fm-3m space group, a = 5.1442 ± 0.0005 Å), and α-$A1_2O_3$ powder contains two phases with rhombohedral (R-3c space group, a = b = 4.7690 ± 0.0005 Å, c = 13.0220 ± 0.0033 Å) and monoclinic (P2 space group with lattice parameters a = 9.5558 ± 0.0078 Å, b = 5.1294 ± 0.0040 Å, c = 9.1620 ± 0.0103 Å) structures.

Al content of up to 5% in NiAl has no effect on the XRD pattern of Ni (only slightly shifting the peak to the left, a = 3.5249 ± 0.0003 Å). An increase in the Al content by up to 15% leads to the displacement of the main peak in the Ni diagram with the occurrence of reflexes of intermetallic compound $AlNi_3$ (Pm-3m, a = 3.5712 ± 0.0003 Å).

2.2 *Preparation of Porous Samples of Tubular Shape by APS Method*

Mechanical mixtures of the oxide powders Al_2O_3 or 9.5YSZ and Ni or nickel alloys NiAl in equal weight proportions were used for preparation of the sample of tubular shape by the air plasma spraying (APS) method [7]. The spraying was done by a semiautomatic APS industrial set using air plasma spray-type UMP-7 apparatus and plasma torches of our own design with an external rotating anode. The powder mixtures were deposited on a metal pin 9 mm in diameter with a precoated antiadhesive layer. After spraying, tubular-shaped samples (about 10 mm in diameter and 220 mm in length) were taken off the pin by soaking in water to remove the adhesive layer. The thickness of the tubes' wall was 400–600 μm (Fig. 1). After spraying the porosity of the samples was evaluated by the hydrostatic weighing method and was found to be equal to 20–22%.

The phase content of the samples was examined after deposition, after heat treatment for 2 h at 1350 °C in argon, and after the subsequent reducing in a hydrogen atmosphere for 2 h at 1350 °C. XRD study of the samples was performed using a DMAX-2500 with Ni-filtered CuK_α radiation in the range of $25^\circ \leq 2\theta \leq 85^\circ$. The surface morphology of the samples was studied by a scanning electron microscope Auriga Crossbeam Workstation (Carl Zeiss) combined with an INCA SEM MA System. The electrical conductivity of the samples was measured by the four-point

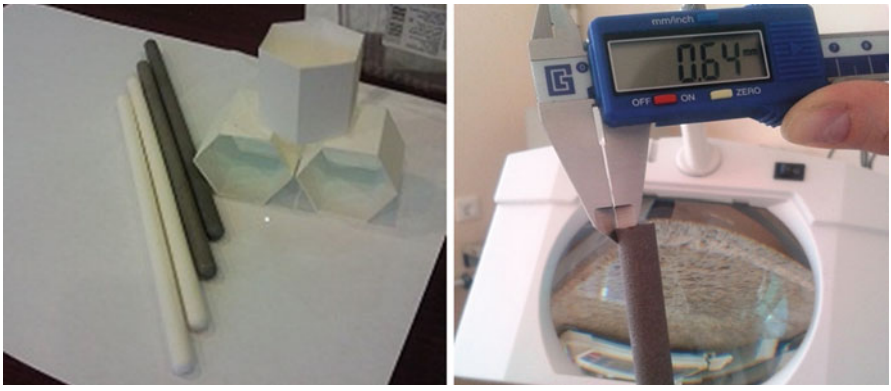

Fig. 1 Porous samples of tubular shape fabricated by APS method (white samples made from Al_2O_3, dark – from the cermets)

DC technique in hydrogen using a microprocessor system ZIRCONIA-318. Thermal expansion of samples in air and argon was studied using a dilatometer Tesatronic TT60.

3 Results and Discussion

3.1 Structure and Phase Changes After Heat Treatment

In as-sprayed Ni + 9.5YSZ samples, the oxide phase $Zr_{0.758}Y_{0.242}O_{1.879}$ with a cubic structure and a lattice parameter a = 5.1479 ± 0.0003 Å and metallic nickel (a = 3.5272 ± 0.0003 Å) were detected together with a small amount of 1.9 wt.% NiO (a = 4.1828 ± 0.0007 Å). The composition was stable during heat treatment in different atmospheres. After firing in argon with following reduction in hydrogen, NiO was completely reduced up to the metallic state (Fig. 2a).

Replacing nickel with $Ni_{95}Al_5$ is marked by a slight shift of the Ni and 9.5YSZ peaks to a smaller angle area and also by the appearance of a small amount of NiO and $NiAl_2O_4$. When treated in Ar, the nickel oxide was reduced to metallic nickel and the amount of spinel in the samples increased. The activation energy of the reduction reaction of NiO in the temperature 291–509 °C range is 18 kJ mol^{-1} and that of the reduction reaction of spinel in 1014–1264 °C range is 134 kJ mol^{-1} [8]. This means that NiO reduces more readily than $NiAl_2O_4$. After reduction in hydrogen, traces of Al_2O_3 were detected in the mixture of Ni and 9.5YSZ (Fig. 2b). In the $Ni_{85}Al_{15}$–9.5YSZ cermet samples, the formation of a remarkable amount of $NiAl_2O_4$ and $Al_{0.14}Ni_{0.86}$ (cubic structure Fm-3m, a = 3.5491 ± 0.0003 Å) was found after spraying. Treatment in argon led to the appearance of non-stoichiometric spinel which, after reduction in hydrogen, transformed into metal nickel and alumina (Fig. 2c).

After being held in argon, the samples changed in colour from grey to green and also significantly increased in size (by 7.4%) which was not observed in the other compositions based on 9.5YSZ. After reducing in hydrogen, the samples' sizes differed from their original state by only 0.3%. During heating in hydrogen, the changes in sample sizes were less remarkable.

In the case of Ni-Al_2O_3, after spraying the main phases were metallic Ni, γ-Al_2O_3 phase with a cubic structure (space group Fd-3 m, lattice parameter a = 7.9105 ± 0.0006 Å) and the nuclei of α-phase crystallization (Fig. 3a). After annealing in argon, the γ-Al_2O_3 phase transformed into α-$A1_2O_3$. It should be noted that after spraying in the Al_2O_3-cermet Ni was found mainly in a metallic state, only in the sample Ni-Al_2O_3 was the NiO content found to be about 0.5%.

With the substitution of Ni to NiAl alloys, non-stoichiometric spinel was detected (Fig. 3b, c) in addition to main phases. After Ar treatment it transformed into spinel $NiAl_2O_4$ and after annealing in hydrogen decomposed to Ni and α-$A1_2O_3$ according to the scheme:

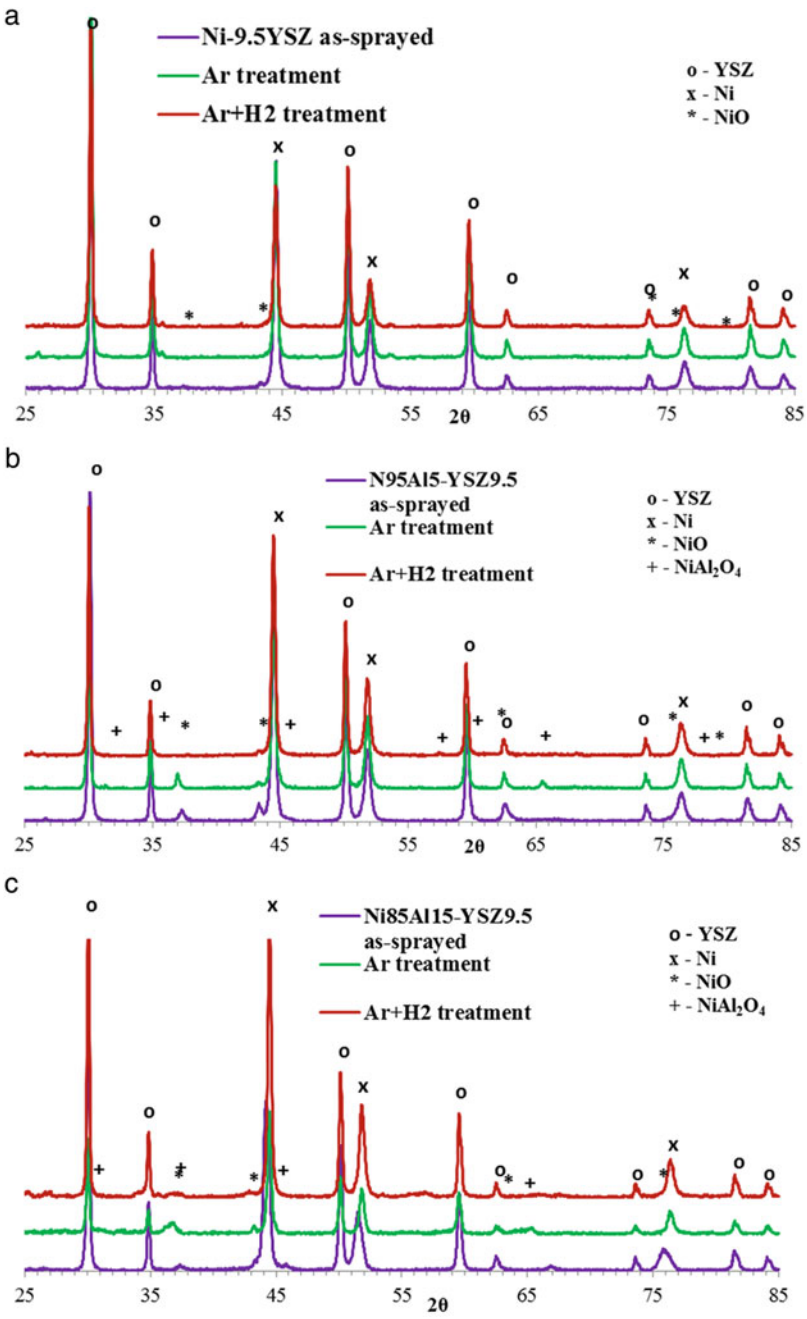

Fig. 2 XRD patterns of the cermet samples based on 9.5YSZ with Ni (**a**) and NiAl alloys $Ni_{95}Al_5$ (**b**) and $Ni_{85}Al_{15}$ (**c**)

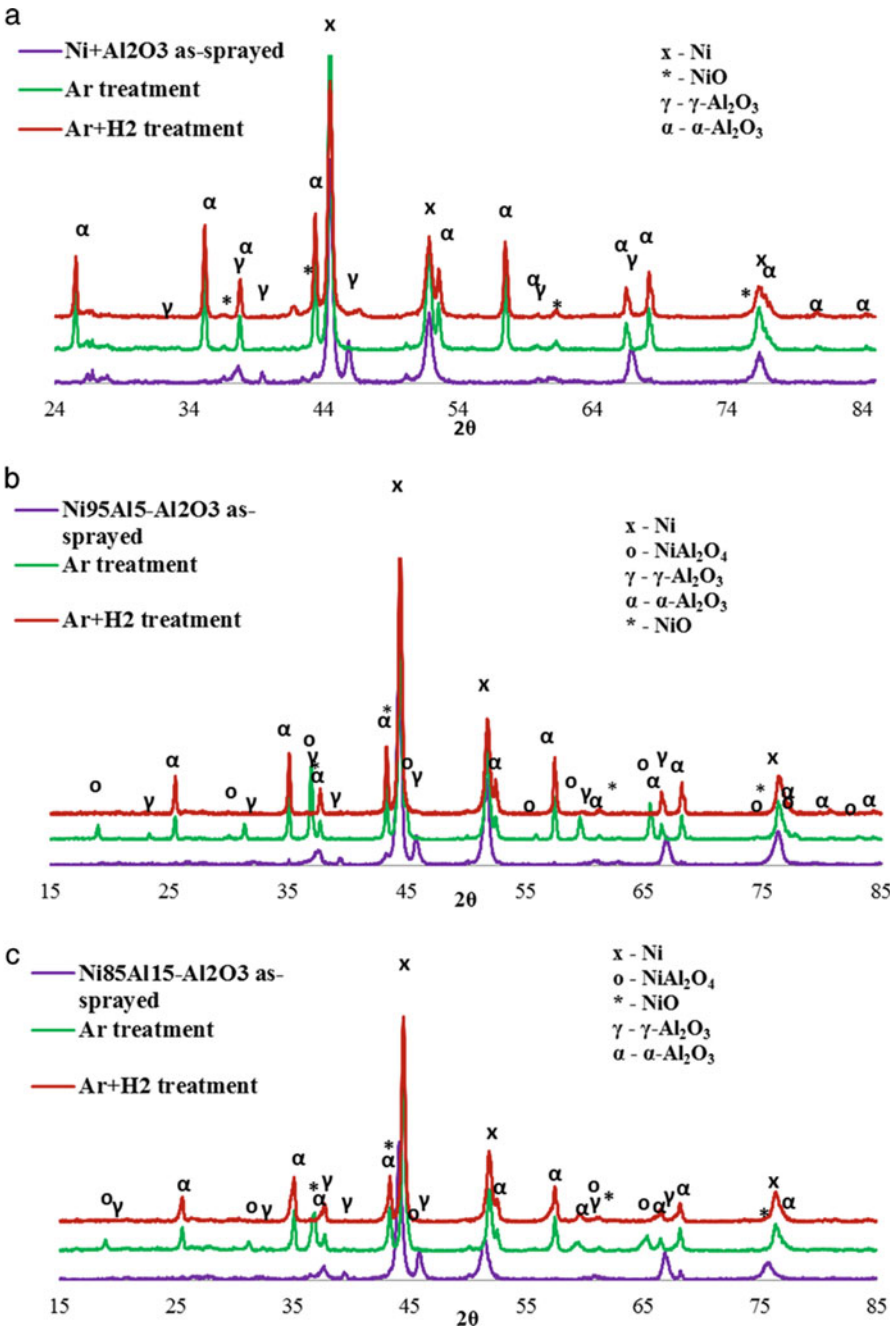

Fig. 3 XRD patterns of the cermet samples based on Al_2O_3 with Ni (**a**) and NiAl alloys $Ni_{95}Al_5$ (**b**) and $Ni_{85}Al_{15}$ (**c**)

$$Ni_2Al_{18}O_{29} \rightarrow {}^{T,Ar} \rightarrow NiAl_2O_4 \rightarrow {}^{T,H}{}_2 \rightarrow Ni + Al_2O_3 + H_2O \uparrow .$$

The colour of all Al_2O_3-based samples changed from grey to green under an Ar atmosphere and then again became grey after reducing in H_2. The most significant change in size among the composites based on alumina was found for $Ni_{85}Al_{15}$-Al_2O_3 after Ar treatment, but it was less than that in the case of $Ni_{85}Al_{15}$–9.5YSZ.

3.2 Electrical Properties of the Cermets

Electrical properties of the cermets were investigated in wet hydrogen on the samples after treatment in Ar with following reducing in H_2. The conductivity of anode cermets with Ni and $Ni_{85}Al_{15}$ measured in wet hydrogen (3% H_2O) ranges from 100 to 150 S/cm at the temperatures of 600–900 °C.

The doping of Ni with Al in the range of solubility (5 mol%) leads to a significant increase in conductivity. It shows good electrocatalytic activity for hydrogen oxidation reactions. The maximal value was found to be 1364 S/cm for $Ni_{95}Al_5$-Al_2O_3 cermet at 600 °C, which is in the top range of the values of conductivity of the usual Ni-cermet anodes presented in the literature [9].

After reducing Ni-9.5YSZ in a hydrogen atmosphere, it was found that the Ni in the ceramic matrix formed into relatively large isolated particles, and this could be a possible reason for their reduced contact and conductivity (Fig. 4a, b). The substitution of Ni by nickel alloy in YSZ-based cermet and the use of Al_2O_3 as a ceramic base prior to heating in an oxidizing atmosphere led to the formation of thin barriers of Al_2O_3 and/or $NiAl_2O_4$ on the surface of the deposited layers. In a reducing atmosphere, this films break up into fine Ni and Al_2O_3 preventing the consolidation of nickel particles (Fig. 4c, d). An increase in Al content of up to 15% in the NiAl alloy above the solubility limit leads to the appearance of nonreversible compounds such as $AlNi_3$ which may be the reason for a further reduction in conductivity.

3.3 Thermal Expansion

The dependence of the thermal expansion of Ni-9.5YSZ during heating in air and in Ar was non-linear with a sharp increase in the high-temperature interval. The calculated CTE values were 8.4×10^{-6} K^{-1} (25–630°C), 31.3×10^{-6} K^{-1} (630–730°C) and 58.6×10^{-6} K^{-1} (730–900°C), respectively. The same extreme expansion was observed for all samples with YSZ ceramic matrix regardless of the metallic component. It is probably connected with Ni oxidation by residual oxygen in commercial argon. However, in our investigations, Al_2O_3-based cermets demonstrated even expansion under the same conditions across all temperature ranges. Calculated CTE values of $Ni_{95}Al_5$-Al_2O_3 change smoothly from 9.1 to 11.1×10^{-6} K^{-1} in the range of 25–900°C.

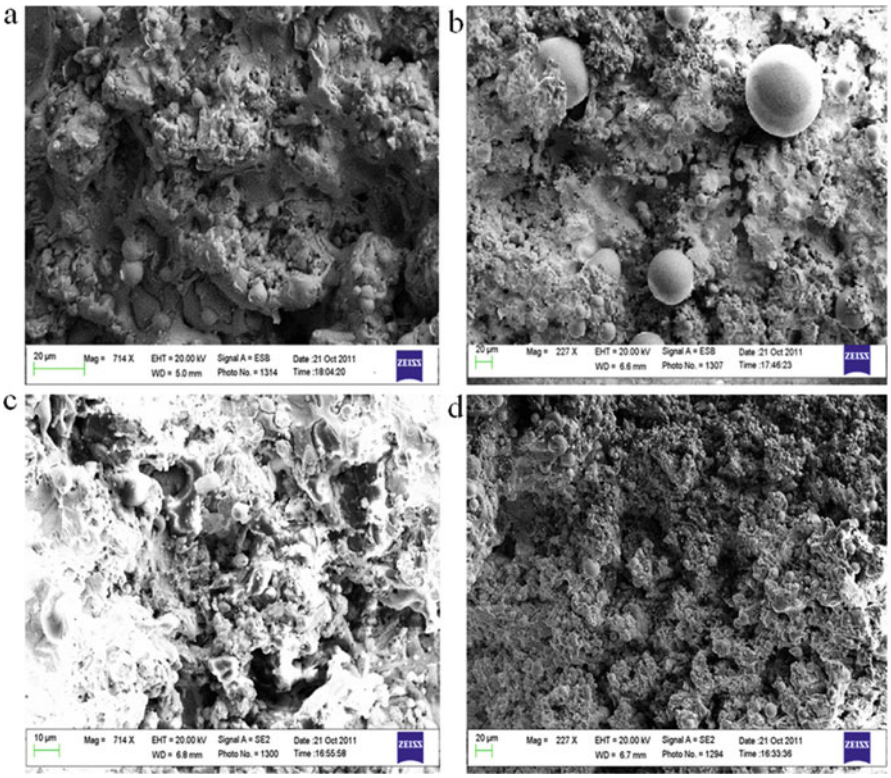

Fig. 4 Microstructure of cermets after spraying and after reducing in H_2: (**a**, **b**) Ni-9.5YSZ; (**c**, **d**) $Ni_{95}Al_5$-Al_2O_3

4 Conclusions

In order to form porous composite anodes of tubular shape by the air plasma spraying method, mechanical mixtures of the oxide powders Al_2O_3 or 9.5 YSZ and metal alloys $Ni_{100-x}Al_x$ (x = 0; 5; 15) were utilized in equal weight proportions. It was found that, after spraying, Ni and its alloys remain mainly in a metallic state. When substituting Ni with nickel alloys and using Al_2O_3 as a ceramic base under heating in an oxidizing atmosphere, a thin protective layer of Al_2O_3 and/or $NiAl_2O_4$ formed on the surface of deposited particles. In a reducing atmosphere, this film breaks up into fine Ni and alumina preventing the consolidation of nickel particles. The positive effect of such substitution is an increase in conductivity (1364 S/cm and 644 S/cm at 600 °C in hydrogen for Al_2O_3 + $Ni_{95}Al_5$ and 9.5YSZ + $Ni_{95}Al_5$, respectively) and reduced expansion of the samples. During heating in argon, the CTE of Al_2O_3 + $Ni_{95}Al_5$ changed smoothly from 9.1 to 11.1 × 10^{-6} K^{-1} in the

range 25–900°C. The cermet having Al_2O_3 + $Ni_{95}Al_5$ content is a preferred candidate among the investigated cermets for further usage as a supporting anode in SOFC production.

Acknowledgements The present work was supported by Act 211 Government of the Russian Federation, contract № 02.A03.21.0006.

References

1. Hui, R., Wang, Z., Kesler, O., Rose, L., Jankovic, J., Yick, S., Maric, R., Ghosh, D.: Thermal plasma spraying for SOFCs: Applications, potential advantages, and challenges, review. J. Power Sources. **170**, 308–323 (2007)
2. Cowin, P.I., Petit, C.T.G., Lan, R., Irvine, J.T.S., Tao, S.: Recent progress in the development of anode materials for solid oxide fuel cells. Adv. Energy Mater. **1**(3), 314–332 (2011)
3. Shiratori, Y., Teraoka, Y., Sasaki, K.: $Ni_{1-x-y}Mg_xAl_yO$–ScSZ anodes for solid oxide fuel cells. Solid State Ionics. **177**(15–16), 1371–1380 (2006)
4. Orui, H., Chiba, R., Nozawa, K., Arai, H., Kanno, R.: High temperature stability of alumina containing nickel-zirconia cermets for solid oxide fuel cell anodes. J. Power Sources. **238**, 74–80 (2013)
5. Sadykov, V.A., Usoltsev, V.V., Fedorova, Y.E., et al.: Design of medium–temperature solid oxide fuel cells on porous supports of deformation strengthened Ni–Al alloy. Russian J. Electrochem. **47**(4), 488–493 (2011)
6. Pikalov, S.M., Polukhin, V.A., Kuznetsov, I.A.: Correlation of electromagnetic and mechanical properties of functional plasma sprayed coatings and criterion of non-destructive control quality. Metally. **6**, 146–152 (1995)
7. Pikalov, S.M., Selivaniv, E.N., Chumarev, V.M., Pikalova, E.Yu., Zaikov, Yu.P., Ermakov, A. V.: Composite electrode material for electrochemical devices. Patent Ru № 2523550, 20.07.2014
8. Sridhar, S., Sichen, D.U., Seetharaman, S.: Investigation of the kinetics of reduction of nickel oxide and nickel aluminate by hydrogen. Z. Met. **85**, 616–620 (1994)
9. Tsipis, E.V., Kharton, V.V.: Electrode materials and reaction mechanisms in solid oxide fuel cells: A brief review. J. Solid State Electrochem. **12**(11), 1367–1391 (2008)